# Progress in Performance Improvement and New Research Areas for Cost Reduction of 2G HTS Wires

V. Selvamanickam, Y. Chen, I. Kesgin, A. Guevara, T. Shi, Y. Yao, Y. Qiao, Y. Zhang, Y. Zhang, G. Majkic, G. Carota, A. Rar, Y. Xie, J. Dackow, B. Maiorov, L. Civale, V. Braccini, J. Jaroszynski, A. Xu, D. Larbalestier, and R. Bhattacharya

***Abstract*—Second-generation (2G) HTS wires are now being produced routinely in kilometer lengths using Metal Organic Chemical Vapor Deposition (MOCVD) process with critical currents of 300 A/cm. While this achievement is enabling several prototype devices, in order to reach a substantial commercial market, the cost-performance metrics of 2G HTS wires need to be significantly improved in device operating conditions. Zr-doping has been found to be an effective approach to improve in-field critical current performance of MOCVD-based HTS wires. In this work, we have explored modifications to the Zr-doped precursor compositions to achieve three and two-fold increase in deposition rate in research and production MOCVD systems respectively. Production wires made with modified Zr-doped compositions exhibit a self-field critical current density of 50 $\mathrm{MA/cm^2}$ at 4.2 K and a 55 to 65% higher performance than our previous wires with Zr-doping, over magnetic field range of 0 to 30 T. We have also developed an alternate, low-cost technique, namely electrodeposition, to deposit silver overlayer on superconducting film. Wires made with electrodeposited silver are able to sustain the same level of overcurrent as sputtered silver layers. This process has been successfully scaled up to 100 m lengths.**

***Index Terms*—BZO, critical current, electrodeposition, magnetic field, MOCVD, second-generation HTS, silver, Zr.**

## I. Introduction

SECOND-GENERATION (2G) $\mathrm{REBa_2Cu_3O_x}$ (REBCO, $\mathrm{RE}$ = rare earth) High Temperature Superconducting (HTS) wires have been scaled up to pilot-scale manufacturing and are produced routinely in lengths of more than a kilometer. Our 2G HTS wire consists of biaxially-textured buffers based on ion beam assisted deposition (IBAD) of MgO [1]–[3] on high-strength Hastelloy substrates followed by REBCO film deposition by metal organic chemical vapor deposition (MOCVD) [4], [5]. The use of IBAD to achieve biaxially-textured template has several benefits including choice of essentially any substrate. Such a choice allows us to employ high-strength, non magnetic and high resistivity substrates. High-strength substrates provide a great benefit in device fabrication, especially for high-field magnets. Additionally, thin (50 $\mu\mathrm{m}$) substrates are possible because of high strength which results in substantially higher engineering current density. Non magnetic and high resistivity substrates lead to lower ac losses. Metal Organic Chemical Vapor Deposition is the only technique that has been used to demonstrate 2G HTS wires longer than a kilometer. A world-record performance of 300,330 A-m was demonstrated over a 1,065 m long wire in 2009 using MOCVD [6]. While the ability to manufacture a complex thin film using epitaxial growth over lengths of kilometer is impressive, a major factor that needs to be addressed to reach widespread commercial use of 2G HTS wire is its cost. The feedback from device manufacturers indicates that 2G HTS wire price of less than $ 50/kA-m in *device operating conditions* needs to be achieved for a substantial commercial market. So, our research in the last year has been focused on improving the cost-performance metrics of 2G HTS wire in device operating conditions. In addition to higher zero-field critical current ($\mathrm{I_c}$) at 77 K, the performance of the wire in a magnetic field of a few Tesla is an important factor that affects the cost-performance metric. In this paper, we will present advances made in improving the in-field performance of MOCVD-based 2G HTS wires and the successful transition to production. Additionally, we will introduce an alternate technique to deposit silver overlayer, namely electrodeposition as a low-cost alternative to vacuum deposition processes such as sputtering that are commonly used. While the content of silver in 2G HTS wire is small ($< 2\ \mu\mathrm{m}$), silver deposition is an important constituent of wire cost as well as production capacity.

Manuscript received August 03, 2010; accepted December 20, 2010. Date of publication February 22, 2011; date of current version May 27, 2011. This work was supported by a Contract with the US Department of Energy. Part of the work at NHMFL was also supported by the National Science Foundation.

V. Selvamanickam, I. Kesgin, A. Guevara, T. Shi, Y. Yao, Y. Zhang, Y. Zhang, and G. Majkic are with the Department of Mechanical Engineering and the Texas Center for Superconductivity, University of Houston, Houston, TX 77204 USA.

Y. Chen, Y. Qiao, G. Carota, A. Rar, Y. Xie, and J. Dackow are with SuperPower, Schenectady, NY 12304 USA.

B. Maiorov and L. Civale are with Los Alamos National Laboratory, Los Alamos, NM 87545 USA.

V. Braccini, J. Jaroszynski, A. Xu, and D. Larbalestier are with the National High Magnetic Field Laboratory, Florida State University, Tallahassee, FL 32306 USA.

R. Bhattacharya is with the National Renewable Energy Laboratory, Golden, CO 80401 USA (e-mail: selva@uh.edu).

Digital Object Identifier 10.1109/TASC.2011.2107310

## II. Improved Critical Currents in Magnetic Fields

In 2009, we demonstrated more than two-fold improvement in critical current of MOCVD-based (Gd,Y)-Ba-Cu-O (GdYBCO) films using Zr-doping [7], [8]. Zr-tetra methyl heptanedionate (thd) was added to the precursor solution for Zr doping [7], [8]. $\mathrm{BaZrO_3}$ (BZO) nanocolumns formed by a self-assembly process were found to be responsible for improved pinning. BZO-based self-assembled nanocolumnar structure had been previously created by several groups using pulsed laser deposition [9]–[12] to achieve improved pinning, but it was not obvious that a similar structure could be achieved by a chemical process where Zr is added to the precursor rather than BZO to the PLD target. After demonstrating that it

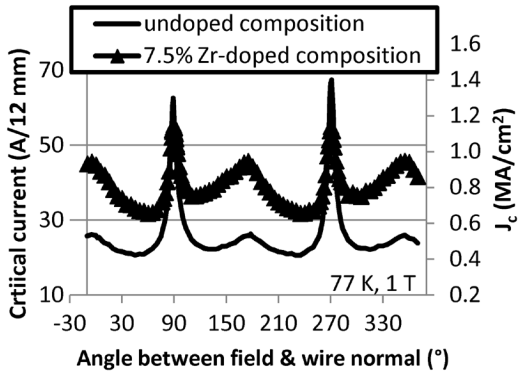


Fig. 1. Angular dependence of critical current of 0.4 $\mu$m thick films fabricated in research MOCVD system using undoped and Zr-doped precursors.

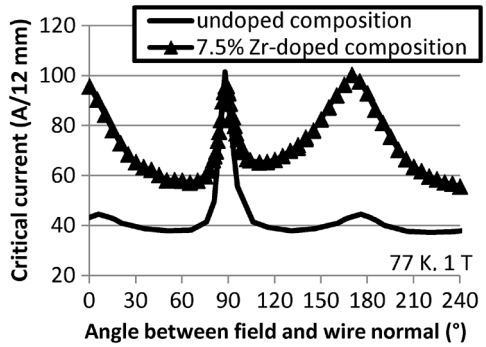


Fig. 2. Angular dependence of critical current of 1.1 $\mu$m thick films fabricated in production MOCVD system using undoped and Zr-doped precursors.

is indeed possible with MOCVD, optimization of Zr content in the GdYBCO film resulted in the highest critical current at a Zr doping level of 7.5%. Also, in 2009, we were able to successfully transition the process to manufacturing [13]. Figs. 1 and 2 show the angular dependence of critical current of GdYBCO wires made in research and production MOCVD systems with and without Zr-doping. A two-fold improvement in critical current is observed over a wide angular range with Zr doping in both research and production systems. The higher magnitude of critical current in the production system is due to the fact that the films were 1.1 $\mu$m in thickness compared to 0.4 $\mu$m thick films fabricated in the research MOCVD system.

While superior in-field performance has been achieved with Zr-doped precursor chemistry, a drawback was the need to reduce the deposition rate in the MOCVD process. In the research MOCVD system, a deposition rate of 0.13 $\mu$m/min was used in fabrication of the Zr-doped wire that is described in Fig. 1, which is 1/4 of the deposition rate that is normally used in this system. In order to explore if compositional changes could be made to improve the deposition rate, we embarked on a thorough investigation of rare-earth precursor composition in GdYBCO films at a fixed Zr doping level of 7.5%. We found that even with a fixed Zr-doping level, the in-field performance can be substantially modified by changing the Gd+Y content or the Gd:Y ratio [14]. In addition, in this work, we evaluated the influence of Ba:Cu content of the starting precursor. We found that with a starting precursor chemistry of $Y_{0.6}Gd_{0.6}Ba_{2.0}Cu_{2.3}O_x$, a high in-field critical current can be achieved even at a three-fold higher deposition rate of 0.4 $\mu$m/min. Fig. 3 displays the

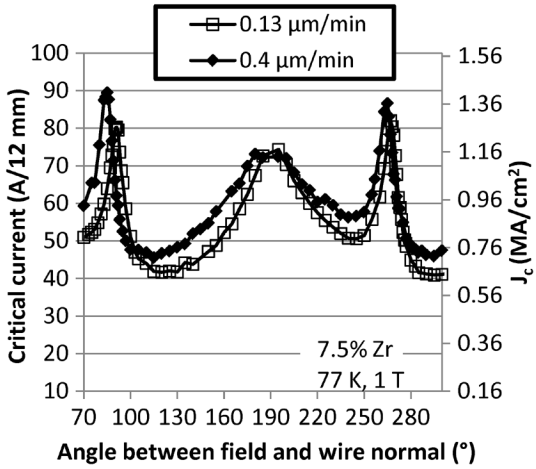


Fig. 3. Angular dependence of critical current of 0.5 $\mu$m thick films fabricated in research MOCVD system using Zr-doped precursors with two different compositions and different deposition rates.

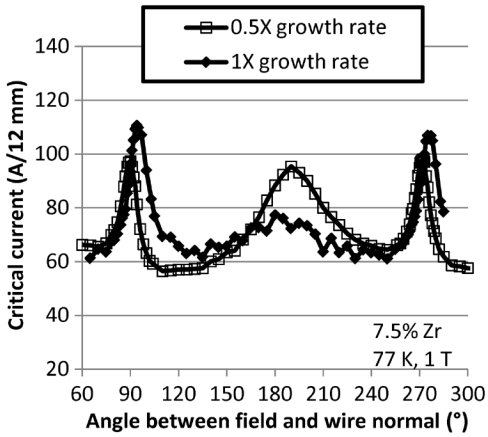


Fig. 4. Angular dependence of critical current of 1.1 $\mu$m thick films fabricated in production MOCVD system using Zr-doped precursors with two different compositions and different deposition rates.

angular dependence of critical current of a sample with a starting precursor composition of $Y_{0.65}Gd_{0.65}Ba_{2.0}Cu_{2.3}O_x$ processed at a deposition rate of 0.13 $\mu$m/min and the angular dependence of critical current of a sample with a starting precursor composition of $Y_{0.6}Gd_{0.6}Ba_{2.0}Cu_{2.3}O_x$ processed at a deposition rate of 0.4 $\mu$m/min. It is seen that in both cases, the critical current performance is very similar. The reason for achieving good critical current even at a higher deposition rate is not clear, but a high density of self-assembled BZO nanocolumns were observed in the high-rate samples too, indicating that the self-assembly process could be sustained even at a high deposition rate using the modified composition.

The Zr-doped precursor chemistry with the modified precursor composition was then transferred to the production MOCVD system. We were able to confirm that high in-field critical currents could be achieved even with a high deposition rate in the production MOCVD system using the modified precursor composition. Fig. 4 shows angular dependence of critical current of two wires made with the original and modified compositions, the same as was used in the samples made in the research system. It is seen that even at twice the deposition rate, the in-field performance of the wire fabricated using the

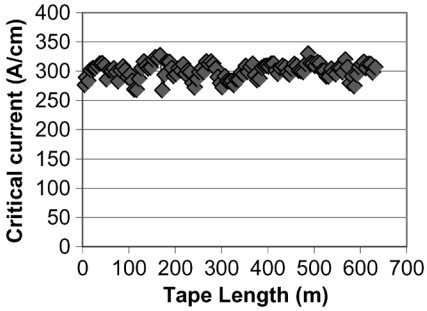


Fig. 5. Transport critical current measured every 5 m of a 600 m long wire fabricated by MOCVD using modified Zr-doped composition.

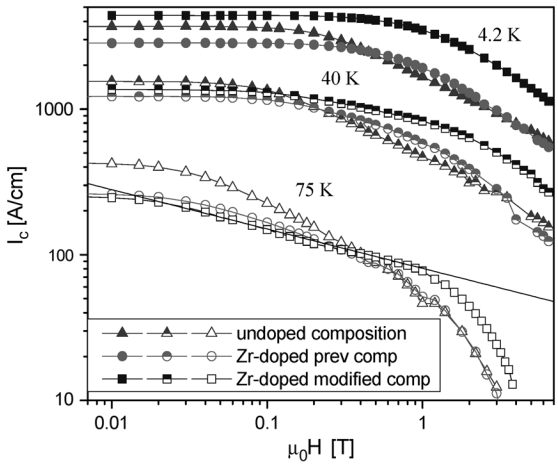


Fig. 6. Magnetic field dependence of critical current of wires made in production MOCVD system using undoped and Zr-doped compositions. Measurements were done with field along the wire normal and at 4.2 K, 40 K, and 75 K.

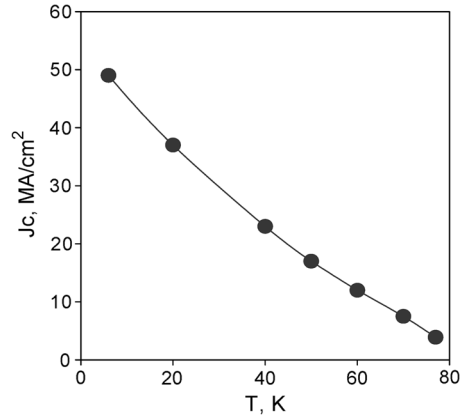


Fig. 7. Temperature dependence of self-field critical current density of wires made in production MOCVD system using modified Zr-doped composition.

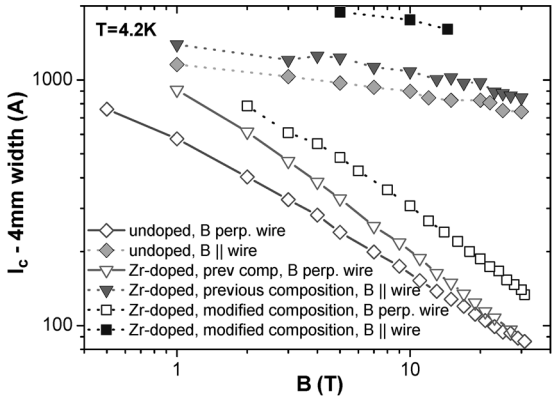


Fig. 8. Magnetic field dependence of $\mathrm{I_c}$ of wires made in production MOCVD system using undoped and Zr-doped compositions. Measurements were done with field parallel and perpendicular to the wire, at 4.2 K.

modified composition is comparable with that made using the original composition. The critical current in the orientation of field along the wire normal $(\mathrm{B} \parallel \mathrm{c})$ is lower in the case of the wire fabricated at a higher rate. But, the critical currents in the orientation of field perpendicular to the wire normal $(\mathrm{B} \perp \mathrm{c})$ and the minimum critical current values are comparable in both wires. The minimum critical current value is typically the key parameter that determines the performance of HTS devices in most applications. Since a high value of minimum critical current is achievable even at a higher deposition rate, we can realize the benefit of the faster production process and still meet application requirements.

Wires are now manufactured in the production MOCVD system using the modified composition. Uniformly good critical current values between 250 to 300 A/cm are routinely produced with the modified Zr-doped composition. The zero-field critical current of a 600 m long wire made in the production MOCVD with the modified Zr-doped composition is shown in Fig. 5. A uniformly high critical current can be observed over the entire wire length.

The in-field performance of production wires made with modified Zr doped composition have been measured over a temperature range of 4.2 K to 77 K and magnetic field range of 0 to 30 T. Fig. 6 shows the critical current density values of wires fabricated in the production MOCVD system without Zr doping and with Zr doping with previous and modified precursor compositions. It is seen that the new production wires exhibit the best critical current over the entire range of magnetic fields up to 7 T at 4.2 K. The new production wires show the highest critical current values above 0.2 T at 40 K and above 0.5 T at 75 K. So, the production wires made with the modified composition display the best performance at essentially all field values that are relevant in practical applications. It is also seen from Fig. 6 that the $\alpha$ value of the wire made with the modified Zr-doped composition is low at 0.27 at 75 K.

A similar set of production wires without Zr doping and with Zr doping, the latter using the original and modified GdYBCO compositions were examined at 4.2 K, in the orientation of $\mathrm{B} \parallel$ wire and $\mathrm{B} \perp$ wire from 0 to 30 T. All wires had a nominal superconductor film thickness of 1.1 $\mu\mathrm{m}$. The zero-field critical current of a recent production wire with modified Zr-doped composition over a temperature range of 4.2 K to 77 K is shown in Fig. 7. This wire sustained a zero-field critical current density of 3 $\mathrm{MA/cm^2}$ (310 A/cm) (at 77 K which increased to 50 $\mathrm{MA/cm^2}$ at 4.2 K. Results from in-field measurements from the three wires are shown in Fig. 8. Consistent with the results shown in Fig. 6, the recent production wires with modified Zr-doped composition show the best critical current performance over the entire magnetic field range of 0 to 30 T and in both field orientations.

The critical current values of the Zr-doped wires at 5 T and 10 T at $\mathrm{B} \parallel$ wire and at 10 T and 20 T at $\mathrm{B} \perp$ wire are summarized

TABLE I
CRITICAL CURRENT OF PRODUCTION MOCVD WIRES MADE WITH ORIGINAL AND MODIFIED Zr-DOPED COMPOSITIONS

| $I_c$ @ 4.2 K in field (A/4 mm) | Previous composition | Modified composition |
|---|---|---|
| 10 T, B $\perp$ wire | 201 | 310 |
| 20 T, B $\perp$ wire | 118 | 183 |
| 5 T, B $\parallel$ wire | 1,219 | 1,893 |
| 10 T, B $\parallel$ wire | 1,073 | 1,769 |

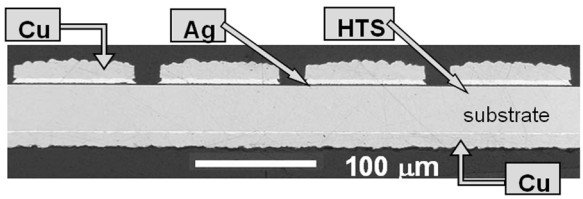


Fig. 9. Cross section of a multifilamentary 2G HTS wire with superconductor film, silver and copper stabilizer all striated.

in Table I. As shown in the table, the recent Zr-doped wires have yielded a 55 to 65% higher critical current at these high magnetic fields.

## III. SILVER ELECTRODEPOSITION

The typical thickness of silver in 2G HTS wire is only about 2% of the overall wire architecture. However, the capacity of 2G HTS wire production and wire cost are impacted the silver layer especially since vacuum deposition techniques such as magnetron sputtering are typically used. In this work, we explored an alternate, lower-cost technique for silver overlayer, namely electrodeposition. Since the copper stabilizer in our wire architecture is also deposited by electrodeposition, this would allow for both silver and copper to be deposited in tandem, which can lead to a further reduction in processing cost. Another important benefit of electrodeposition is in the fabrication of multifilamentary 2G HTS wire for low ac losses. While techniques are being developed to fabricate striated 2G HTS wire, it is important that the silver overlayer and copper stabilizer are also striated. A cross section of a previously fabricated 2G HTS wire with superconductor film, silver overlayer and copper stabilizer all striated is shown in Fig. 9. It is not a straightforward task to achieve such an architecture especially over long lengths. Clearly, etching techniques will not be economical to striate a thick copper stabilizer. Therefore, it is desirable to fabricate an all-striated architecture without having to etch a thick copper stabilizer. Once a striated superconducting film is fabricated, a vacuum deposition process such as silver sputtering will couple all the filaments and defeat the purpose of filamentization. On the other hand, since electrodeposition occurs preferentially on low-resistivity areas, a striated silver structure can be obtained on the filamentized superconducting film. Similarly, a striated, thick copper stabilizer can be obtained by preferential deposition on the striated silver layer. Hence, electrodeposition can be an enabling technique to fabricate a fully filamentized 2G HTS wire.

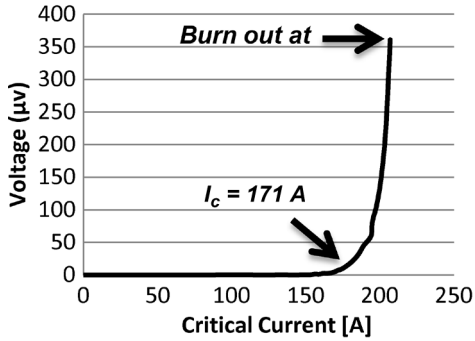


Fig. 10. Current-voltage characteristic of a 2G HTS wire with electrodeposited silver overlayer until burn out.

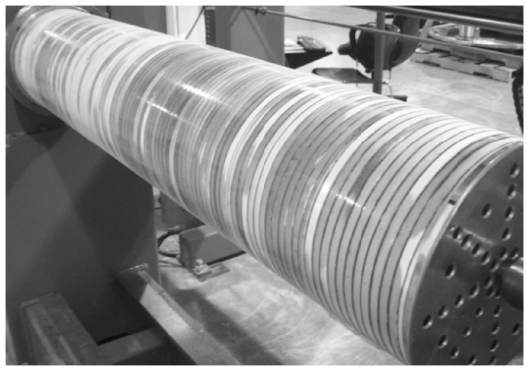

Fig. 11. Photograph of a 100 m long, 12 mm wide HTS wire made with electrodeposited silver on superconducting film.

In this work, we explored silver electrodeposition on superconducting films using silver nitrate solution. A silver thickness of approximately 2 $\mu$m was used. An important metric in the quality of silver layer is the contact resistivity with the superconducting film. Contact resistance measurements were done on a wire with electrodeposited silver using a three-probe technique and a resistivity value of 4 $\mu\Omega\mathrm{cm}^2$ was measured. This value is higher than that of sputtered silver contacts. So, in order verify the effectiveness of the silver overlayer, we conducted overcurrent measurements until burn out of the wire. Fig. 10 shows a current-voltage curve obtained from one such measurement. It is seen that the sample with about 2 $\mu$m of electrodeposited silver is able to sustain 20% higher current beyond the take-off current. This value is comparable with that measured in samples with sputtered silver indicating the functionality of the electrodeposited silver.

Next, we evaluated if the electrodeposition process can be scaled up to long lengths. A 100 m long 2G HTS wire, 12 mm in width was electrodeposited with silver at a tape speed of 20 m/h in the same research-scale system that was used for short sample fabrication. Fig. 11 shows a photograph of the 100 m wire wound on a mandrel.

Non contact critical current measurements were conducted using hall-probe technique over the 100 m before and after electrodeposition, and after oxygenation and the results are summarized in Fig. 12. Overall, it is seen that the critical current stays

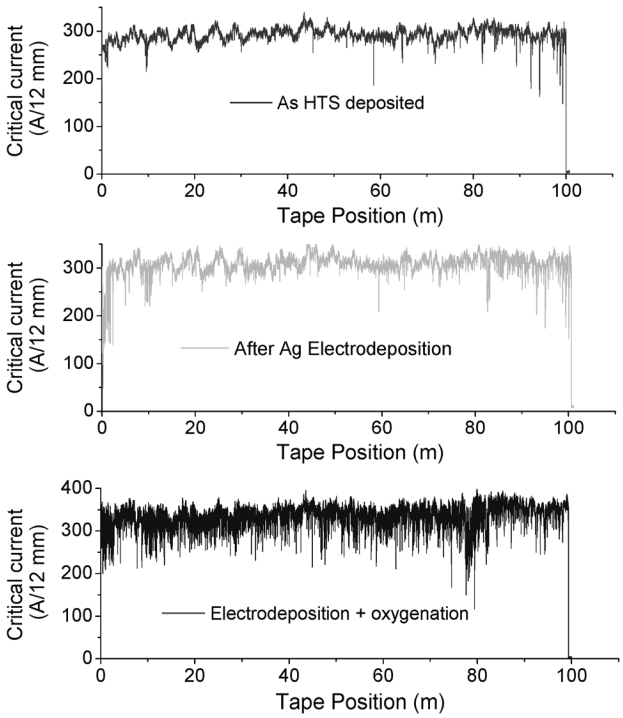


Fig. 12. Non contact critical current measurements obtained from a 100 m long, 12 mm wide HTS wire made with electrodeposited silver on superconducting film.

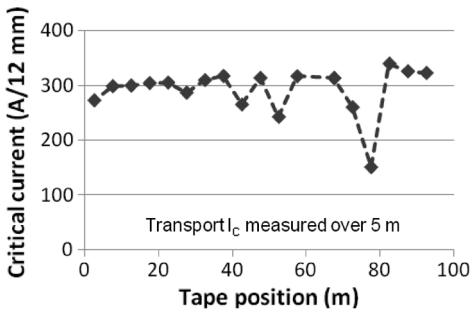


Fig. 13. Transport current current measurements obtained from a 100 m long, 12 mm wide HTS wire made with electrodeposited silver.

at the 300 A level over the 12 mm width after each step indicating no degradation in the wire quality after the electrodeposition and oxygenation processes. It is to be noted that the spatial resolution along the wire length in these non contact measurements is 1 mm, as a result of which more details are seen in the critical current values. In order to probe the efficacy of the silver coating, contact measurements were conducted over the 100 m using transport current four-probe technique. Data was obtained at every 5 m interval and the results are shown in Fig. 13. The transport critical current values are found to be consistent with the results from non contact measurements, with an average critical current of 300 A over the 12 mm width. The critical current drops to a lower value at 80 m which could be due to a discontinuity problem that occurred during the electrodeposition process. The ability to flow transport current over the 100 m length shows that the electrodeposited silver-superconductor interface is good for current transfer and that the silver

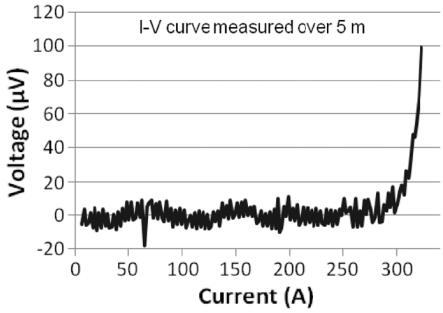


Fig. 14 Current-voltage curve obtained from transport current measurements over a 5 m segment of a 100 m long HTS wire made with electrodeposited silver.

surface is good enough for pressed electrical contacts which are used in the transport current measurement system.

A current-voltage curve from one of the 5 m segments that was measured is shown in Fig. 14. It is seen that the wire was able to sustain 10 to 20% higher current beyond the take-off current value without wire burn out, up to the maximum measurement voltage of 100 $\mu$V (0.2 $\mu\mathrm{V/cm}$). This data reconfirms the efficacy of the electrodeposited silver even when processed in a continuous reel-to-reel mode over 100 m.

## REFERENCES

[1] C. P. Wang, K. B. Do, M. R. Beasley, T. H. Geballe, and R. H. Hammond, "Deposition of in-plane textured MgO on amorphous $\mathrm{Si_3N_4}$ substrates by ion-beam-assisted deposition and comparisons with ion-beam-assisted deposited yttria-stabilized-zirconia," *Appl. Phys. Lett.*, vol. 71, p. 2955, 1997.

[2] J. R. Groves, P. N. Arendt, H. Kung, S. R. Foltyn, R. F. DePaula, L. A. Emmert, and J. G. Stover, "Texture development in IBAD MgO films as a function of deposition thickness and rate," *IEEE Trans. Appl. Supercond.*, vol. 11, p. 2822, 2001.

[3] X. Xiong, S. Kim, K. Zdun, S. Sambandam, A. Rar, K. P. Lenseth, and V. Selvamanickam, "Progress in high throughput processing of long-length, high quality and low cost IBAD MgO and buffer tapes at superpower," *IEEE Trans. Appl. Supercond.*, vol. 19, p. 3319, 2009.

[4] V. Selvamanickam, Y. Xie, J. Reeves, and Y. Chen, "MOCVD-based YBCO-coated conductors," *Mater. Res. Soc. Bull.*, vol. 29, p. 579, 2004.

[5] V. Selvamanickam, Y. Chen, X. Xiong, Y. Y. Xie, M. Martchevski, A. Rar, Y. Qiao, R. M. Schmidt, A. Knoll, K. P. Lenseth, and C. S. Weber, "High performance 2G wires: From R&D to pilot-scale manufacturing," *IEEE Trans. Appl. Supercond.*, vol. 19, p. 3225, 2009.

[6] V. Selvamanickam, Y. Xie, and J. Dackow, in *Proc. High Temperature Superconductivity Program Peer Review*, Alexandria, VA, August 4–6, 2009 [Online]. Available: http://www.htspeerreview.com/2009/pdfs/presentations/day%201/joint/2-Joint-Progress-in-SuperPowers-2G-HTS-Wire-Development-Program.pdf

[7] V. Selvamanickam, Y. Chen, J. Xie, Y. Zhang, A. Guevara, I. Kesgin, G. Majkic, and M. Martchevsky, "Influence of Zr and Ce doping on electromagnetic properties of (Gd,Y)-Ba-Cu-O superconducting tapes fabricated by metal organic chemical vapor deposition," *Physica C*, vol. 469, p. 2037, 2009.

[8] Y. Chen, V. Selvamanickam, Y. Zhang, Y. Zuev, C. Cantoni, E. Specht, M. Paranthaman, T. Aytug, D. Lee, and A. Goyal, "Enhanced flux pinning by $\mathrm{BaZrO_3}$ and $\mathrm{(Gd,Y)_2O_3}$ nano-structures in metal organic chemical vapor deposited (GdY)BCO high temperature superconductor wires," *Appl. Phys. Lett.*, vol. 94, p. 062513, 2009.

[9] J. L. Macmanus-Driscoll, S. R. Foltyn, Q. X. Jia, H. Wang, A. Serquis, L. Civale, B. Maiorov, M. E. Hawley, M. P. Maley, and D. E. Peterson, "Strongly enhanced current densities in superconducting coated conductors of $\mathrm{YBa_2Cu_3O_{7-x}} + \mathrm{BaZrO_3}$," *Nature Materials*, vol. 3, p. 439, 2004.

[10] S. Kang, A. Goyal, J. Li, A. A. Gapud, P. M. Martin, L. Heatherly, J. R. Thompson, D. K. Christen, F. A. List, M. Paranthaman, and D. F. Lee, "High-performance high- $\mathrm{T_c}$ superconducting wires," *Science*, vol. 311, p. 1911, 2006.

[11] Y. Yamada, K. Takahashi, H. Kobayashi, M. Konishi, T. Watanabe, A. Ibi, T. Muroga, S. Miyata, T. Kato, T. Hirayama, and Y. Shiohara, "Epitaxial nanostructure and defects effective for pinning in $\mathrm{Y(RE)Ba_2Cu_3O_{7-x}}$ coated conductors," *Appl. Phys. Lett.*, vol. 87, p. 132502, 2005.

[12] M. Mukaida, T. Horide, R. Kita, S. Horii, A. Ichinose, Y. Yoshida, O. Miura, K. Matsumoto, K. Yamada, and N. Mori, "Critical current density enhancement around a matching field in $\mathrm{ErBa2Cu3O7} - \delta$ films with $\mathrm{BaZrO_3}$ nano-rods," *Jpn. J. Appl. Phys.*, vol. 44, p. L952, 2005.

[13] V. Selvamanickam, A. Guevara, Y. Zhang, I. Kesgin, Y. Xie, G. Carota, Y. Chen, J. Dackow, Y. Zhang, Y. Zuev, C. Cantoni, A. Goyal, J. Coulter, and L. Civale, "Enhanced and uniform in-field performance in long (Gd, Y)-Ba-Cu-O tapes with zirconium doping fabricated by metal-organic chemical vapor deposition," *Supercond. Sci. Technol.*, vol. 23, p. 014014, 2010.

[14] Y. Chen, T. Shi, A. P. Guevara, Y. Zhang, Y. Yao, I. Kesgin, and V. Selvamanickam, "Composition effects on the critical current of MOCVD-processed Zr:GdYBCO coated conductors in an applied magnetic field," *IEEE Trans. Appl. Superconduct.*, vol. 21, no. 3, Jun. 2011.